Abdelrahim *et al.*
Journal of Electrical Systems and Inf Technol (2022) 9:13
https://doi.org/10.1186/s43067-022-00052-3

Journal of Electrical Systems and Information Technology

RESEARCH Open Access

RF performance evaluation of the nRF24L01+ based wireless water quality monitoring sensor node: Khartoum city propagation scenario

Sami Omer Osman Abdelrahim*, Mohamed Zakria Mohamed Hassan, Alzain Mohamed Suliman Salih, Amjed Abubaker Mohamed Abdo-Alrahiem and Mayada Abdelgadir Mohamed

*Correspondence: eng.samiosman@outlook.com

Electronics Engineering Department, Sudan University of Science and Technology, Khartoum, Sudan

Abstract

Recently, and to cater to increased needs of Drinking Water Quality Monitoring (DWQM) and data management, there has been a growing interest in the marketplace as well as in the research community to develop advanced water quality monitoring systems utilizing modern information and communications technologies (ICT) such as wireless sensor networks (WSN) and Internet of Things (IoT). The application of the wireless-sensing paradigm is becoming a common trend in water quality monitoring systems. In fact, a growing body of the literature has focused on developing wireless sensing-enabled water quality monitoring systems. However, previous studies have not dealt with the radio performance evaluation of modern wireless water quality monitoring systems deployed in urban city scenarios. The present paper seeks to address the radio frequency (RF) performance evaluation for a developed modern wireless Drinking Water Quality Monitoring System (DWQMS) based on the commercial nRF24L01+ RF module. This research study is based on three city propagation scenarios as case studies. The obtained experimental data suggested that the nRF24L01+ module can provide relatively acceptable RF performance under less favorable and hostile city propagation environments.

Keywords: WSN, IoT, nRF24L01+ transceiver, RF performance evaluation, Propagation modeling, Free-space, Two-ray, Log-distance, Drinking water quality monitoring system (DWQMS)

Introduction

Water is considered an important limited and critical resource over the world. This significant resource is essential for agriculture, industry, and creatures' existence on earth including human beings. Nowadays, smart solutions for water quality monitoring are gaining importance with advancements in communication technology. The introduction of such a system paves the way for a wide range of applications such as drinking water monitoring, municipal and industrial wastewater monitoring, and environmental water monitoring (rivers, lakes, groundwater, and oceans) [1].

Over recent years, WSNs have received considerable attention in environmental, industrial monitoring, and control applications. Practical deployment of WSNs requires the evaluation of path loss values between the different network nodes using proper propagation models [2]. A propagation model is essentially an empirical mathematical equation used to abstract and predicts wave propagation through the radio channel and to estimate the maximum path loss experienced within this channel, from which the minimum acceptable signal level and, hence, the maximum transmission distance can be estimated [3, 4]. Generally, a propagation model aims to estimate the average received signal strength (which is spatially variable) considering specific parameters and factors (e.g., Line-of-Sight (LOS) propagation, reflection, and diffraction) that approximately characterize wave propagation over the radio channel [3, 4]. Based on this, it is possible to experimentally investigate wave propagation across a wireless sensor system by collecting sufficient samples of measured RF data [2, 3] and employing a suitable path loss model that can be used to estimate the characteristics and predict the level of signals traversing the media among the sensor nodes and, hence, be able to reliably plan and design a wireless system that will be able to cope with hostile media and maintain an acceptable level of error performance and signal-to-noise ratio (SNR) [2–8]. The study of radio propagation varies across different clutter areas (rural, suburban, and urban) [3]. Another consideration to bear in mind during propagation modeling is whether the wireless system is to be deployed indoors or at an outdoor premise [3]. Furthermore, for WSN application scenarios, which mainly utilize short-range communication protocols, some constraints should be taken into account during propagation modeling: 1) low energy consumption: the transmitted power is restricted in the WSN systems (e.g., the defined power is 1 mW set by IEEE 802.15.4 standard). 2) Low antenna heights: sensor nodes are nearly close to the ground. 3) Directivity: omnidirectional antennas are usually used in the WSN system [2–6].

The subject wireless system of this study is a DWQMS developed based on the WSN paradigm, and it consists mainly of three parts: branch node, central node/base station, and a communication system between nodes. The branch (or sensor) node consists of sensors that are used to collect water quality data and transmit it to the central node. On the other hand, the central node acts as a monitoring and controlling unit that houses a local database, a graphical user interface (GUI) to visualize and analyze the received data and then notify the consumer. For the communication between the sensing nodes, wireless connectivity is realized based on the nRF24L01+ module. In addition, the system also incorporates a Wi-Fi module used to transmit data to an online cloud platform, providing the feature of monitoring and logging sensors data through the Internet. Local monitoring at the central node is also made possible using a computer GUI to which a copy of the sensor nodes data is sent using a local Universal Asynchronous Receiver Transmitter (UART) serial communications port at the central node.

This study aims to examine and evaluate the radio performance of a WSN-based DWQMS deployed in an urban propagation environment via carrying out a field experiment under varying scenarios and conditions.

The remaining part of this paper proceeds as follows: "Literature review" section presents a review of relevant research work, and "Methods" section gives a brief review of the architecture employed in the design of the proposed system, in addition to the

hardware and software design methods. "The proposed setup and experimental results" section includes a description of the proposed experimental scenarios together with a discussion of the various results obtained thereof. Our conclusions, as well as a summary of the principal findings, are drawn in "Conclusions" section.

Literature review

Considerable efforts have been done by researchers, companies, and authorities for developing modern DWQM systems that enable consumers and public authorities to monitor the quality of drinking water. A substantial and growing body of the literature has studied the development of modern low-cost and efficient water quality monitoring systems [9–20]. However, even though a vast amount of the literature is available, few studies have been published on the radio performance evaluation aspects of modern wireless DWQM systems. A review of some of the more recent and relevant studies is introduced in the following paragraphs.

A preliminary version of this work was carried out and appeared in [9]. In this article, we present an approach to building an effective low-cost, real-time, and in situ DWQMS using the open-source Arduino microcontroller. Additionally, our work included a detailed performance evaluation of the proposed DWQMS under typical household conditions within the city of Khartoum.

In [7], the authors proposed a radio propagation model for WSN based on the Free-space path loss equation to be used in tracking and localization applications. Four components of path loss were taken into account to contribute to the prediction of the received signal levels, which are: free-space, ground reflection, received signal strength uncertainty, and antenna radiation pattern irregularity. The results of the model have been tested and verified using Tmote Sky sensor nodes which employed a 2.4 GHz CC2420 radio module and an internal inverted-F antenna. The proposed model was able to forecast the received signal strength within a specified distance.

Salient efforts were conducted in [2], to provide a comprehensive comparison among the various types of propagation models being used in the design of WSN. Authors have demonstrated the state of the art in WSN path loss modeling corroborated with quantitative comparisons of different models under different scenarios and frequency bands. They concluded that employing proper WSN path loss modeling is imperative in the design and performance evaluation of WSNs, additionally; they affirmed that the exploitation of unsuitable path loss models could lead to improper design and erroneous results. Hence, to arrive at reasonable results during the design and analysis of WSNs, and before using a specific model, it is of extreme importance to study the applicable scenarios and the constraints of the respective model.

Other efforts were done in [10]. The authors designed an efficient IoT-enabled DWQMS that aims to reduce power consumption via a simple design method. They used TI CC3200 ARM Microcontroller Unit (MCU) as the main microcontroller in their design. This special type of microcontroller has a built-in Wi-Fi module. This allowed for reduced power consumption, reduced complexity, and improved speed of operation. Conductivity, turbidity (TU), water level, and potential hydrogen (pH) were selected as quality parameters. The Wi-Fi module was used to transmit data to the "Ubidots" cloud platform, which gives the feature of monitoring and logging sensors data through the

Internet. The programming of the controller was done using "ENERGIA IDE" software. Furthermore, authors have set up an experiment, whereby the quality parameters were measured and sent to the "Ubidots" platform. The measured results were compared with drinking water quality standards which are defined by the World Health Organization (WHO), after which the "Ubidots" platform alerts the consumer with an SMS or e-mail should any abnormal value is detected.

Review work on [13] surveys the application of WSN in environmental monitoring, with a particular focus on water quality. Various WSN-based water quality monitoring techniques suggested by other articles were studied and analyzed, taking into account their coverage, energy, and security aspects. This work also examined, compared, and evaluated different sensor node architectures proposed by various research works in terms of monitored parameters, data security features, MCU type being used, and wireless communication standards being adopted, in addition to power supply architectures, localization capabilities, autonomy, and potential application scenarios.

The paper in [14] describes the “SmartCoast” multi-sensor system for water quality monitoring. The system goal is to provide a platform able of meeting the monitoring requirements of the European Union (EU) Water Framework Directive (WFD) aiming at maintaining good quality status for all ground and surface water bodies. The key parameters under investigation included: phosphate, temperature, conductivity, pH, dissolved oxygen, TU, and water level. The “SmartCoast” system enables easier integration of water quality sensors as required, through exploiting a flexible WSN platform that was developed at Tyndall laboratory.

In [15], the authors analyzed the transmission performance of a WSN in a static indoor test setup consisting of 5 to 14 transmitters and up to 4 receivers. The nRF24L01 transceiver module was used, where it implements the proprietary Adaptive Network Topology (ANT) protocol for WSNs and operates in the 2.4 GHz Industrial, Scientific and, Medical (ISM) band. Tests were conducted in over 500 configurations with different numbers of transmitters, message frequencies, and packet sizes. The experimental tests point out the trade-off between data rate and packet length regarding the impact on the packet loss rate. It was found that using multiple receivers can mitigate and reduce burst packet loss. The achieved results offer valuable insights on the configuration of an application-specific device based on the nRF24L01 module as well as the redundancy methods for maximizing the data throughput.

In summary, it is worth noting that there is a growing interest among the research community to develop modern DWQM systems that aim to improve water quality monitoring efficiency and reduce costs through utilizing recent advancements in ICT technologies including IoT and WSN. In conclusion, overall, the available body of the literature tended to focus on the performance of DWQMs from a non-radio communications perspective, and hence, this highlights the need for more focus and light to be shed on the radio performance aspects of modern wireless DWQM systems.

Methods

To date, a variety of methods have been introduced to develop modern DWQM systems [21]. Most of these methods are quite similar, differing mainly in minor changes or additions [21]. To fulfill the functions of the proposed DWQMS, this work follows the

common practical design approach of dividing the system into two main nodes: a central node and a branch node(s). It is worth mentioning that the proposed system makes use of both IoT and WSN technologies, which makes it more versatile and flexible in terms of its monitoring capability of the desired water bodies/sites. The following subsections include a detailed discussion on the necessary background information as well as a breakdown of the system design methodology.

Branch node

The branch (or sensor) node, as shown in Fig. 1, is the heart of the DWQMS. It acts as the first process in the water quality monitoring cycle and serves as the node responsible for collecting quality data from the desired monitoring site(s). The success or the failure of the entire system heavily depends on the performance of this node. The idea is to install a collection of this branch (or sensor) node in many consumer sites in a spatially distributed manner to form a WSN that will monitor, for instance, the drinking water quality in the water distribution system from the source to the tap. This node, as depicted in Fig. 1, contains all the water quality sensors (pH, TU, electrical conductivity (EC), and temperature sensors) and it also contains a microcontroller (Arduino MCU) that collects the raw sensors' data, processes it, implements the water quality assessment algorithm and also sends data to the base station or central node. Additionally, this node also includes the signal conditioning circuits required to interface with the controller, as shown in Fig. 1. The reason for the inclusion of the signal conditioning circuits

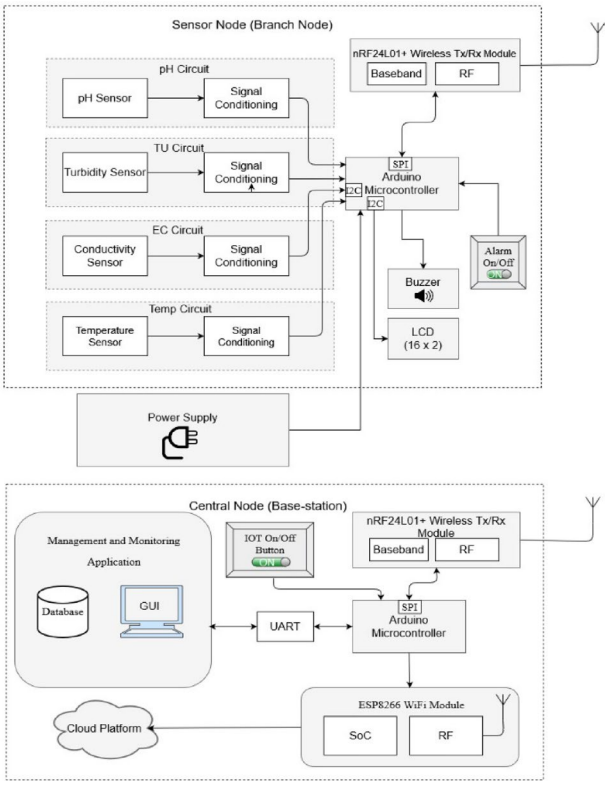

Fig. 1 Proposed DWQM system architecture

is that each sensor produces a signal that needs to be conditioned in some manner to interface with the microcontroller (for instance, conditioning includes amplification and level shifting to fit the sensor output signal within the detectable range for the microcontroller's Analog-to-Digital Converter (ADC)). In addition, to maintain data integrity and obtain accurate results, the MCU takes the average for every 50 consecutive samples for each sensor.

The branch (or sensor) node, as shown in Fig. 1, has provisions for on-site monitoring and notification, including a liquid crystal display (LCD) screen that continuously displays the quality data and a buzzer for audible notification/alarming whenever any quality parameter violates the safety thresholds. A button for switching the audible alarm on/off is also included for more flexibility. The last step for the sensor node before repeating its measurement cycle is to wirelessly convey the collected quality data to the central node using the nRF24L01+ module.

Central node

The central (or base-station) node, on the other hand, mainly functions as a monitoring and a controlling unit. Similar to the sensor node this entity is built around an Arduino MCU, which acts as the brain for this node, as shown in Fig. 1. The Arduino is tasked with the processing of the collected water quality data received from the sensor node(s) to restructure it in a suitable format for other data management functions. On top of data processing, Arduino also provides a copy of the same quality data to a local GUI developed using Python programming language. The GUI is linked to a local database built around SQL-Lite, which facilitates sensor nodes' data storage and management. Additionally, a copy of the same GUI data is uploaded to the "Ubidots" online IoT cloud platform via the ESP8266 Wi-Fi module. For improved user experience, the end-user is given the liberty to turn the Ubidots online data monitoring feature on/off via a button embedded onto the central node.

To sum up, the central node, as depicted in Fig. 1, acts as the interface through which the end-user/operator is provided with: remote and real-time data visualization, analysis (via the Python-based GUI), storage, management, and visual notification (GUI pop-up messages upon detecting abnormal quality conditions at a sensor node location). Additionally, besides monitoring and visualization, the GUI also enables the user to control the quality parameters threshold values as well as the sampling frequency of the remote sensor node(s), thereby increasing the system flexibility.

Communication between nodes

As its name implies, a wireless sensor network is in essence a network of small sensing nodes distributed over an area, where they wirelessly communicate and cooperate to monitor a physical phenomenon within that area [22]. Then, it follows that a fundamental component needed to fulfill the functions of the wireless node is the RF module. Although many types of modules have been introduced in the literature to route data across the different nodes in a WSN [22, 23], there must be a compromise between cost, ease of use, and reliability when choosing the appropriate RF module for a particular application [23]. Subsequently, and after considering all the feasible options, the nRF24L01+ module was chosen for several reasons, for besides its low

Table 1 nRF24L01+ module main features [24]

Radio features	Worldwide 2.4 GHz ISM band operation
	126 different RF channels
	Modulation is based on GFSK (Gaussian frequency shift keying)
	Adjustable data rate (250 kbps, 1 Mbps, or 2 Mbps)
Non-radio features	Programmable output power (0, − 6, − 12 or − 18 dBm)
	1 to 32 bytes dynamic payload length
	Enhanced ShockBurst (ESB)™ protocol
	Ultra-low-power operation and 5 V input tolerance

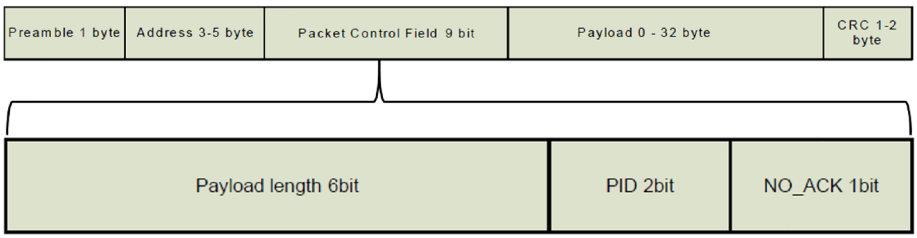

Fig. 2 Enhanced ShockBurst™ Packet Format [24]

cost and reliability it has a multitude of features and diverse applications that the vendor guarantees. Table 1 shows the main features of the nRF24L01+ module [24].

The nRF24L01+ module, as outlined in Table 1, is a single-chip 2.4 GHz half-duplex transceiver that implements the proprietary ESB protocol, which features automatic packet handling through the data link layer [24]. Hence, as this module is half-duplex, it can be set to act as either a transmitter (TX) or a receiver (RX) at a time. Due to the optimized design of the module, it minimizes the need for external components to just an MCU and gives the benefit of high performance, and yet ultra-low power consumption [24]. To fully understand the communication behavior between nodes in the proposed system, some aspects of the nRF24L01+ must be outlined in detail as follows [24]:

Enhanced ShockBurst™ Packet Format Data conveyed between nRF24L01+ modules are encapsulated in a specified ESB packet format, as shown in Fig. 2, which contains: a preamble, address, packet control field, payload (raw data), and Cyclic Redundancy Check (CRC) which is compulsory for error detection.

The first byte of the packet is the preamble, which is a sequence of bits used for receivers' synchronization. The address field, on the other hand, is used to distinguish different receivers by establishing a logical link addressing scheme for each module in such a way that a hypothetical or logical data pipeline between TX and RX modules is formed. This address is configurable and dynamic in length, which can be 3, 4, or 5 bytes long. The third field of the packet, as shown in Fig. 2, is the packet control field, which is 9 bits long. The first 6 bits in this field specify the payload length, the next 2 bits hold the Packet Identity (PID) which is used to detect if a packet is a new or retransmitted packet [24] and also determines the number of retransmissions of each packet, the final bit within PID holds the

no-acknowledgment flag which is used in conjunction with the auto-acknowledgment feature [24] to determine whether the received packet is to be auto acknowledged for the transmitter or not. The fourth field of the ESB Packet is the payload, which is the actual user's data to be transmitted. This field is dynamic and ranges from 0 to 32 bytes. However, it is worth noting that typically, the 0-byte size payload is used in case of acknowledgment packets sent back to the TX. The last field of the packet is the CRC, which is either 1 or 2 bytes and is used for error detection. The value of the CRC is calculated over the address, packet control, and payload fields.

Auto Packet Handling Features A key feature of the nRF24L01+ module is its support for auto packet handling ability, where the microcontroller just needs to push the data to input ports of the module, after which it automatically performs the rest of low-level processing, such as packet assembling, addressing, and CRC calculations [24]. Auto handling process reveals itself through the following features [24]:

Static and Dynamic Payload Length ESB protocol offers either dynamic payload length, where transmitted payloads can have different sizes- or static payload length where all transmitted payloads have the same size. The size of the static payloads can be configured by controlling internal module registers.

Automatic Packet Assembly Before data transmission, the MCU provides the module with the configured address and the payload, where the module automatically generates the preamble, CRC, and forms the complete ESB radio packet to be sent.

Automatic Packet Validation The nRF24L01+ module only works with the ESB packet format shown in Fig. 2, therefore and in the receiving mode, the module is continuously seeking packets with a valid address matching its own configured address, before immediately starting the packet validation process using the PID and CRC fields.

Automatic Packet Disassembly Following the packet validation, the built-in ESB protocol engine automatically disassembles the packet, extracts the user data from the payload field, and provides it to the MCU, which can then be utilized in further processing.

MultiCeiver Feature MultiCeiver [24] stands for "Multi Receiving" where one module when being configured in the receiving mode can receive data from up to 6 transmitters simultaneously, as shown in Fig. 3. The idea of receiving is simple, by using a unique addressing scheme between the transmitter and the receiver a sort of "logical channel" is constructed within the physical RF channel. The receiver makes use of a set of internal registers for storing multiple data without overwriting it [24]; therefore, one receiver can easily receive and store data from multiple transmitters.

Finally, to evaluate and test the performance of the proposed design, various experimental scenarios were conducted under varying operating conditions and environments.

The proposed setup and experimental results

This section examines a field experiment that was carried out to evaluate the wireless communication performance of the wireless link between the sensor and central nodes based on the nRF24L01+ module in the proposed DWQMS. The setup and principal findings of this experiment are discussed in the following subsections.

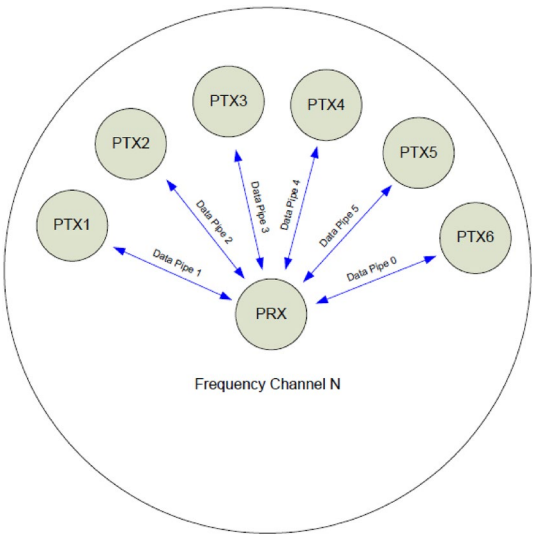

Fig. 3 MultiCeiver™ Feature [24]

Table 2 Experimental parameters

Parameter	Value
Date rate	250 Kbps
Module TX power	0 dBm (Max. Power)
O/p power (including power amplifier (PA) power)	20 dBm
TX and RX Antenna Gains	2 dBi
RX sensitivity (including low-noise amplifier (LNA) gain)	− 104 dBm
Payload size	23 Bytes
Address length	5 Bytes
CRC length	2 Bytes
Frequency	2.519 GHz (Channel no. 119)

City propagation scenarios and parameters

In an attempt to provide a thorough investigation on the performance of the nRFL024 + module applied to DWQM applications, an experimental test setup was proposed and carried out in different scenarios under various RF propagation environments. Furthermore, RF performance was evaluated in terms of the following different metrics: Packet Drop Ratio (PDR), actually utilized throughput, transmission delay, expected receive signal levels, and maximum transmission range.

In this work, two nRF24L01 + modules incorporated within two sensor nodes (where one acts as a master and the other as a slave), two Personal Computers (PCs), and two Arduino MCUs were used. Both of the Arduino MCUs were powered directly from the PCs via USB cables. The relevant parameters of this experimental test setup are summarized in Table 2.

As stated earlier, to provide a reliable assessment of the RF performance of the nRF24L01 + module, this experiment involved three test scenarios that were carried out in two different urban city locations, each having its unique RF propagation characteristics.

Fig. 4 First test scenario (Umm Dawm Street, Al-Jerif East)

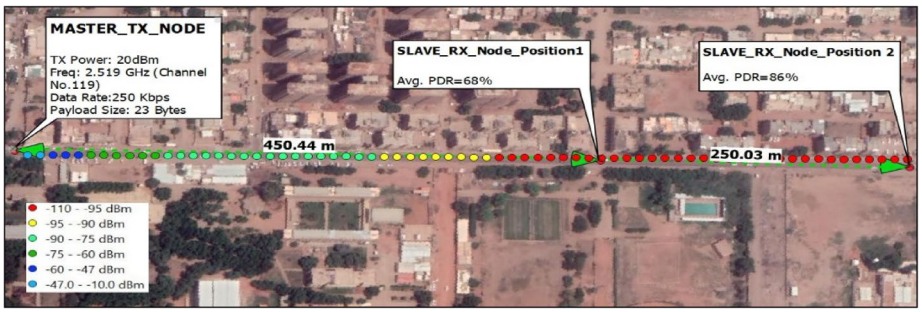

Fig. 5 Second and third test scenarios (Sudan University Southern Campus, Street 61)

The first scenario, as shown in Fig. 4, took place in "Um-Dawm" Street which is located in the city of Khartoum. While the second and third scenarios were performed in Street 61 (near the southern campus of Sudan University of Science and Technology), as shown in Fig. 5.

The three scenarios, as evident from Figs. 4 and 5, involved keeping the master node fixed while moving the slave node over three distances (300, 400, and 700 m) and observing the link reliability in terms of the number of packets lost. In all these scenarios, 23-bytes long payloads were continuously sent from the slave to the master module. The results of each of these test scenarios were recorded in a Comma Separated Values (CSV) file after which they were formatted, analyzed, and visualized using Microsoft Excel, Python programming language, and MATLAB, respectively.

Actual utilized throughput

The actual payload data rate is lower than the advertised rate of 250 kbps due to the overhead bits present in the ESB packet. Assuming ideal conditions where packets can be sent constantly (no delay in between) with 100% packets success, the actual payload throughput (in kbps), denoted by $\overline{\gamma}$, can be calculated as (where k is the payload size, R_p no. of received payloads, and D is the delay):

$$\overline{\gamma} = \frac{K \sum_{m=1}^{n} R_m^p}{D} \tag{1}$$

In this experiment, the actual throughput is 179 Kbps according to the parameters in Table 1. This corresponds to 71.6% utilization of the over-the-air data rate. In fact, at the absolute best utilization (which can be achieved using the ShockBurst (SB)™ mode), 32 data bytes with 4 bytes of overhead can be sent. This gives 88.9% utilization or 222.2 kbps of actual data rate.

Transmission delay

Transmission delay or latency is one of the most important parameters when characterizing the performance of a wireless link, it is also called the time-over-the-air T_{OA} and can be calculated using the following equation:

$$T_{OA} = \frac{M}{R_{OA}} \tag{2}$$

where M is the packet length which equals the payload size added to overhead bits, and R_{OA} is the air data rate. In this experiment, time-over-the-air is 1 ms according to the parameters in Table 2.

PDR

The third performance evaluation was done and measured in terms of the PDR or the packet loss ratio. This parameter is a measure of how many sent packets were lost during transmission, and it can be used as an indicator of the link quality. This value can be calculated by dividing the overall number of packets lost (dropped) at the destination node (D^p) by the overall packet sent from source nodes (S^p) according to:

$$\boldsymbol{PDR} = \frac{\sum_{i=no.des} \boldsymbol{D_i^p}}{\sum_{i=no.sou} \boldsymbol{S_i^p}} \tag{3}$$

Figures 6, 7, and 8 show the PDR achieved in each of the three test scenarios. As can be seen from these Figs., a low average PDR of nearly 0.1% was achieved in the first scenario where the slave and master nodes were separated by approximately 300 m in an area having good LOS conditions. However, as expected, increasing the distance between the slave and master nodes would increase the PDR and, consequently, reduce the link quality. This is demonstrated by the significant increase in the average PDR from 0.1% in the first scenario to about 68% and 86% in the second and third scenarios, respectively.

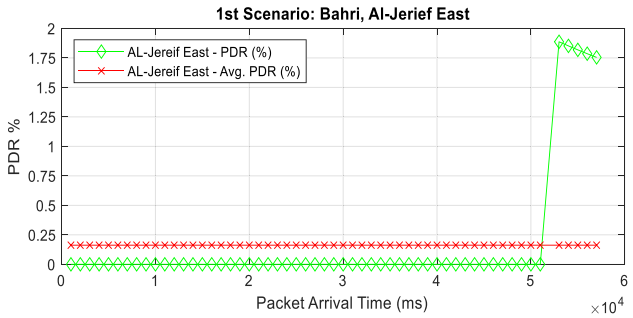

Fig. 6 PDR and received packets as a function of time (1st scenario)

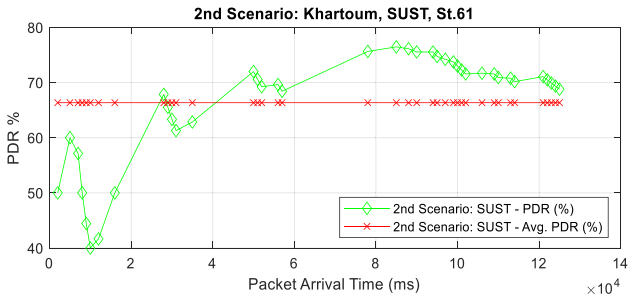

Fig. 7 PDR and received packets as a function of time (2nd scenario)

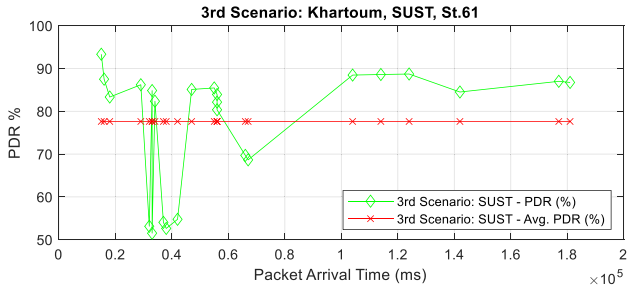

Fig. 8 PDR and received packets as a function of time (3rd scenario)

Additionally, it is worth mentioning that in the latter two scenarios, the propagation environment did not have perfect LOS conditions due to the presence of several obstacles and mobile vehicles, this would seem to justify the large disparities in PDR from the first scenario.

Maximum transmission range

The maximum possible transmission range that could be achieved with the nRF24L01+ module is reportedly quoted as 1 km [25]. However, this maximum range could only be achieved in clear LOS conditions, at the maximum possible output power, and at the minimum data rate [24]. In this experiment, it was observed that 100% PDR (all packets sent were lost) when the transmission distance was increased beyond about 700 m. Consequently, this would seem to imply that for propagation conditions similar to those in the 2nd and 3rd scenarios, the maximum transmission range is in the range from 650 to 700 m.

In order to assess the transmission performance of the nRF24L01+, the signal strength in any of the scenarios needs to be evaluated. As a starting point, an important parameter in estimating the signal strength is the Free-space Loss (FSL), given by [3, 4]:

$$\mathrm{FSL(dB)} = -10\log_{10}\frac{G_T G_R \lambda^2}{16\pi^2 d^2} \tag{4}$$

where G_T and G_R are, respectively, the transmit and receive antenna gains, λ is the wavelength (m), and d is the distance (m) between the transmitter and receiver antennas [3, 4]. Based on the parameters in Table 2, the FSL can be used to predict the received

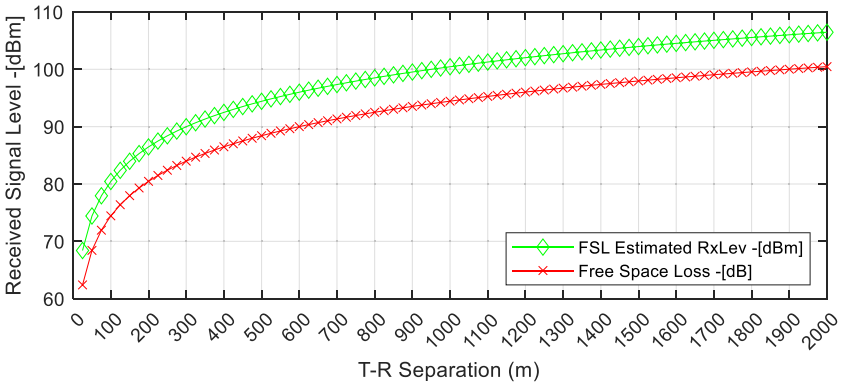

Fig. 9 FSL as a function of distance (carrier Frequency = 2.519 GHz)

signal level over varying TX-RX separations of up to 2 km, as shown in Fig. 9. As can be seen from Fig. 9, at 1 km T–R separation, the FSL model predicts the path loss and received signal level to be around − 94.4 dB and − 100.4 dBm, respectively. Furthermore, according to the same model, the maximum transmission distance for which path loss is acceptable and, accordingly, the receive signal level is within the receiver's sensitivity is estimated to be around 1500–1525 m, which is quite an overly optimistic range compared to practical results attained.

For more accurate prediction and given that the FSL model is overly simplistic and does not consider the effect of urban propagation phenomena such as diffraction, reflection, and scattering on RF signal propagation [4], a plethora of other analytical and empirical RF propagation models can be employed to arrive at more accurate results. A more realistic prediction of path loss and received signal level can be achieved using the widely used two-ray model [3, 4, 6], defined in Eq. 5 below, which considers both the LOS path and the ground-reflected path between the TX and RX:

$$PL(\text{dB}) = 40\log_{10}(d) - (10\log_{10}G_T + 10\log_{10}G_R + 20\log_{10}h_T + 20\log_{10}h_R) \quad (5)$$

where PL is the path loss (in dB), d is the transmitter to receiver distance (m), G_T and G_R are, respectively, the transmitter and receiver antenna gains, h_T and h_R are the transmitter and receiver antenna heights (assumed to be 2 m) [3, 4, 6]. This model predicts the receiver's minimum detectable signal level of − 104 dBm to be within the range of 775–800 m, as shown in Fig. 10.

Another extensively used model in the literature is the log-distance path-loss model which is based on the rudimentary principle of the logarithmic decaying of the received signal level with distance [3, 4]. Based on this model and given the parameters in Table 2, the following path loss model can be derived as follows [3, 4, 6]:

$$PL(d) \propto \left[\frac{d_o}{d}\right]^n \quad (6)$$

$$PL(d) = k\left[\frac{d}{d_o}\right]^{-n} \quad (7)$$

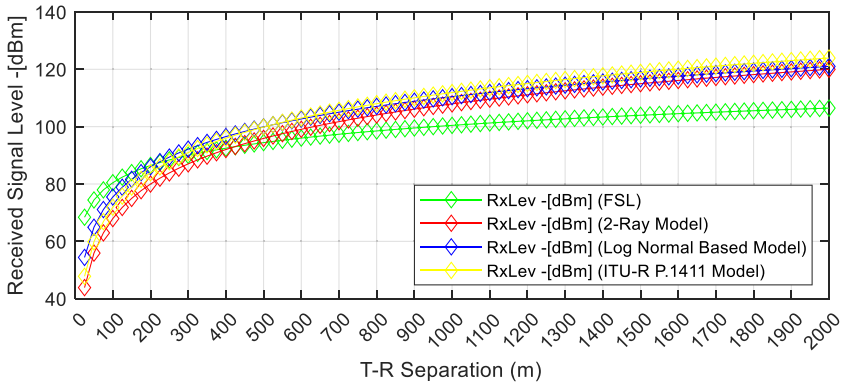

Fig. 10 Predicted Rx level as a function of distance (carrier frequency = 2.519 GHz)

$$PL(d) = k(\text{dB}) - 10n \log_{10}(\frac{d}{d_o}) \tag{8}$$

where k is the proportionality constant (referred to as the reference path loss [4]) and it depends on the channel characteristics and average channel attenuation [3], n is the path loss exponent which depends on the environment and is assumed to be 3.5 as the prevalent environmental conditions closely resemble that of urban cellular systems [3, 6], d_o is a reference distance in the antenna far-field region, and d is the distance between the transmitter and receiver. Validity of this model is only assumed for values of d and d_o that satisfies the following restrictions: $d > d_o$ and $d_o > d_f$ [3, 4], where d_f is the antenna far-field or Fraunhofer distance [4] given by $d_f = 2D^2/\lambda$ whereby D represents the largest antenna dimension which is equal to 61.22 mm in this case. Additionally, provided that omnidirectional antennas are used, the reference path loss (K) is typically assumed to be equal to the FSL at the reference distance d_o [3], and hence, in Eq. (8), it can be substituted by:

$$k(dB) = 20 \log_{10} \frac{\lambda}{4\pi d_o} \tag{9}$$

Given the above constraints and assuming $d_o = 10m$, a straightforward substitution into Eqs. (8) and (9) yields the path loss model given in Eq. 10 below, which is plotted as a function of distance in Fig. 10. From the same data in Fig. 10, it can be seen that this model provides a more accurate estimate of the maximum transmission distance to be within the range of 650–675 m.

$$PL(d) = -60.46 - 35 \log_{10}\left(\frac{d}{10}\right) \tag{10}$$

For the sake of more accurate performance prediction and model comparison, we can make use of another appropriate model proposed by the International Telecommunication Union-Radiocommunication Sector (ITU-R). The model considered herein is one of the ITU-R P.1411-4 recommended models for short-range wireless systems operating in the UHF range under dense-urban or urban conditions [8]. It is characterized by two bounds and a single breakpoint [8], as outlined below:

$$PL(d)_L = L_{bp} + \begin{cases} 20\log_{10}\left(\frac{d}{R_{bp}}\right) & \text{for } d \le R_{bp} \\ 40\log_{10}\left(\frac{d}{R_{bp}}\right) & \text{for } d > R_{bp} \end{cases} \tag{11}$$

$$PL(d)_U = L_{bp} + 20 + \begin{cases} 25\log_{10}\left(\frac{d}{R_{bp}}\right) & \text{for } d \le R_{bp} \\ 40\log_{10}\left(\frac{d}{R_{bp}}\right) & \text{for } d > R_{bp} \end{cases} \tag{12}$$

where $PL(d)_{\mathrm{L}}$ and $PL(d)_{\mathrm{U}}$ are the lower and upper bounds of the predicted path-loss, respectively [8]. While terms R_{bp} and $\mathrm{L_{bp}}$ are, respectively, the breakpoint distance and the corresponding loss at the same distance and are given by [8]:

$$R_{bp} = \frac{4h_T h_R}{\lambda} \tag{13}$$

$$L_{\mathrm{bp}} = \left|20\log_{10}\left(\frac{\lambda^2}{8\pi h_T h_R}\right)\right| \tag{14}$$

where h_T and h_R are the transmitter and receiver antenna heights, respectively [8]. A closer inspection of the predicated receive level based on Eq. (12), shown in Fig. 10, indicates that this model shows noticeable improvements upon the FSL and two-ray models, as it suggests that the maximum transmission distance is within the range 625–650 m.

The data obtained from these models appear to be well supported by the PDR results attained in the previous subsection. This can be clearly shown by referring back to Figs. 4 and 5, where there is a clear trend of weakening receive signal level along the path from the TX to the RX, and a corresponding increase in the PDR, as expected.

Conclusions

The main goal of the present paper was to experimentally evaluate the performance of a proposed wireless DWQMS deployed in the city of Khartoum. The proposed experiment was set out to evaluate the performance of the nRF24L01+based wireless DWQMS nodes at different propagation scenarios and in terms of various metrics including: throughput, delay, PDR, maximum transmission range, and predicted receive levels. The experimental evidence from this study suggested that the nRF24L01+module could have relatively acceptable reliability over considerable transmission ranges. In this paper, we have devised a methodology which can be employed in evaluating the radio performance of a wireless DWQMS based on the commercial low-cost nRF24L01+transceiver. We have also managed to obtain satisfactory results showing that nRF24L01+transceivers are well suited for wireless DWQM systems deployed in urban environments. To sum up, although our results are limited in terms of their generalizability to city scenarios with propagation conditions only similar to those under study, we believe that the obtained empirical figures are showing more than 90% radio performance reliability at distances of around 300 m in good LOS conditions, but only nearly 20–30% radio reliability under hostile non-LOS radio environments that bears a close resemblance to those in the 2nd and 3rd test scenarios. The questions raised by this study are, first if whether the radio performance of nRF24L01+based sensor nodes can be improved

through developing robust routing algorithms in meshed sensor network architecture, and secondly, whether a careful radio survey during the planning phase of DWQM systems wireless node locations could enhance the radio performance of nRFL2401 + transceivers in DWQM systems deployed in city scenarios.

Abbreviations

DWQM	Drinking water quality monitoring
ICT	Information and communication technology
WSN	Wireless sensor network
IoT	Internet-of-things
RF	Radio frequency
DWQMS	Drinking water quality monitoring system
LOS	Line of sight
SNR	Signal-to-noise ratio
GUI	Graphical user interface
UART	Universal asynchronous receiver transmitter
MCU	Microcontroller unit
TU	Turbidity
pH	Potential hydrogen
WHO	World Health Organization
EU	European Union
WFD	Water framework directive
ANT	Adaptive network topology
ISM	Industrial scientific and medical
EC	Electrical conductivity
ADC	Analog–digital-converter
LCD	Liquid crystal display
GFSK	Gaussian frequency shift keying
ESB	Enhanced ShockBurst
TX	Transmitter
RX	Receiver
CRC	Cyclic redundancy check
PID	Packet identity
PDR	Packet drop ratio
PCs	Personal computers
PA	Power amplifier
LNA	Low-noise amplifier
CSV	Comma separated values
SB	ShockBurst
FSL	Free-space loss
ITU-R	International telecommunication union-radiocommunication sector.

Acknowledgements
The authors would like to appreciate and express their deepest gratitude to those who directly and indirectly supported in carrying out this research work.

Author contributions
SOOA worked on the system design, experimental tests, prepared and compiled the results and conclusions. MZMH worked on technical system design and implementation, participated in compiling test results. AMSS and AAMA-A carried out background and literature reviews and assisted in conducting field tests. Finally, MAM provided help in writing and conducting research work. All authors read and approved the final manuscript.

Funding
No funding is provided for this research work.

Availability of data and materials
The datasets used and/or analyzed during the current study are available from the corresponding author on reasonable request.

Declarations

Competing interests
No competing interests.

Received: 27 December 2021 Accepted: 16 May 2022
Published online: 06 June 2022

References

1. U.S. Environmental Protection Agency (2018) Drinking water standards and health advisories. Washington, DC
2. Kurt S, Tavli B (2017) Path-loss modeling for wireless sensor networks: a review of models and comparative evaluations. IEEE Antennas Propag Mag 59:18–37
3. Goldsmith A (2005) Wireless communications. Cambridge University Press, New York
4. Rappaport TS (2002) Wireless communications: principles and practice. Prentice Hall, New Jersey
5. Zhou G, He T, Krishnamurthy S, Stankovic JA (2004) Impact of radio irregularity on wireless sensor networks. In: MobiSys 2004—second international conference on mobile systems, applications and services
6. Taha Al-Wajeeh (2018) Efficient radio channel modeling for urban wireless sensors networks. Université de Poitiers
7. Stoyanova T, Kerasiotis F, Prayati A, Papadopoulos G (2009) A practical RF propagation model for wireless network sensors. In: Proceedings—2009 3rd international conference on sensor technologies and applications, SENSORCOMM 2009
8. Recommendation ITU-R P.1411-9 (2017) Propagation data and prediction methods for the planning of short-range outdoor radiocommunication systems and radio local area networks in the frequency range 300 MHz to 100 GHz
9. Osman SO, Mohamed MZ, Suliman AM, Mohammed AA (2018) Design and implementation of a low-cost real-time in-situ drinking water quality monitoring system using Arduino. In: 2018 international conference on computer, control, electrical, and electronics engineering, ICCCEEE 2018
10. Geetha S, Gouthami S (2016) Internet of things enabled real time water quality monitoring system. Smart Water. https://doi.org/10.1186/s40713-017-0005-y
11. Chowdury MSU, Emran T Bin, Ghosh S, et al (2019) IoT based real-time river water quality monitoring system. In: Procedia computer science
12. Cloete NA, Malekian R, Nair L (2016) Design of smart sensors for real-time water quality monitoring. IEEE Access. https://doi.org/10.1109/ACCESS.2016.2592958
13. Pule M, Yahya A, Chuma J (2017) Wireless sensor networks: a survey on monitoring water quality. J Appl Res Technol. https://doi.org/10.1016/j.jart.2017.07.004
14. O'Flynn B, Martínez-Català R, Harte S, et al (2007) SmartCoast: a wireless sensor network for water quality monitoring. In: Proceedings - conference on local computer networks, LCN
15. Christ P, Neuwinger B, Werner F, Rückert U (2011) Performance analysis of the nRF24L01 ultra-low-power transceiver in a multi-transmitter and multi-receiver scenario. In: Proceedings of IEEE sensors
16. Olatinwo SO, Joubert TH (2019) Energy efficient solutions in wireless sensor systems for water quality monitoring: a review. IEEE Sens J 19:1596–1625
17. Olatinwo SO, Joubert TH (2019) Enabling communication networks for water quality monitoring applications: a survey. IEEE Access. https://doi.org/10.1109/ACCESS.2019.2904945
18. Postolache OA, Silva Girao PMB, Dias Pereira JM, Ramos HMG (2005) Self-organizing maps application in a remote water quality monitoring system. IEEE Trans Instrum Meas. https://doi.org/10.1109/TIM.2004.834583
19. Postolache O, Pereira JD, Girão PS (2014) Wireless sensor network-based solution for environmental monitoring: water quality assessment case study. IET Sci Meas Technol. https://doi.org/10.1049/iet-smt.2013.0136
20. Khutsoane O, Isong B, Gasela N, Abu-Mahfouz M (2020) WaterGrid-sense: a LoRa-based sensor node for industrial IoT applications. IEEE Sens J. https://doi.org/10.1109/JSEN.2019.2951345
21. Dong J, Wang G, Yan H et al (2015) A survey of smart water quality monitoring system. Environ Sci Pollut Res. https://doi.org/10.1007/s11356-014-4026-x
22. Ian F, Akyildiz MCV (2010) Wireless sensor networks, first. Wiley, New York
23. Dargie W, Poellabauer C (2011) Fundamentals of wireless sensor networks: theory and practice. Wiley, New York
24. Nordic (2008) nRF24L01+ Single Chip 2.4GHz transceiver product specification v1.0. Build Res
25. Nilanjan Roy (2021) Long range Arduino based Walkie talkie using nRF24L01. In: https://circuitdigest.com/microcontroller-projects/arduino-walkie-talkie-using-nrf24l01

Publisher's Note